Smart Structures and Systems, *Vol. 16, No. 5 (2015) 807-833*
DOI: http://dx.doi.org/10.12989/sss.2015.16.5.807

Semi-active control of seismic response of a building using MR fluid-based tuned mass damper

Kambiz Esteki[1a], Ashutosh Bagchi[*1] and Ramin Sedaghati[2b]

[1]*Department of Building, Civil, and Environment Engineering, Concordia University, Montreal, Canada, H3G 1M8*
[2]*Department of Mechanical and Industrial Engineering, Concordia University, Montreal, Canada, H3G 1M8*

(Received December 13, 2013, Revised November 28, 2014, Accepted March 1, 2015)

Abstract. While tuned mass dampers are found to be effective in suppressing vibration in a tall building, integrating it with a semi-active control system enables it to perform more efficiently. In this paper a forty-story tall steel-frame building designed according to the Canadian standard, has been studied with and without semi-active and passive tuned mass dampers. The building is assumed to be located in the Vancouver, Canada. A magneto-rheological fluid based semi-active tuned mass damper has been optimally designed to suppress the vibration of the structure against seismic excitation, and an appropriate control procedure has been implemented to optimize the building's semi-active tuned mass system to reduce the seismic response. Furthermore, the control system parameters have been adjusted to yield the maximum reduction in the structural displacements at different floor levels. The response of the structure has been studied with a variety of ground motions with low, medium and high frequency contents to investigate the performance of the semi-active tuned mass damper in comparison to that of a passive tuned mass damper. It has been shown that the semi-active control system modifies structural response more effectively than the classic passive tuned mass damper in both mitigation of maximum displacement and reduction of the settling time of the building.

Keywords: MR damper; tuned mass damper; semi-active tuned mass damper; active tuned mass damper; LQR control system

1. Introduction

Tuned mass dampers (TMD) are passive control devices that are usually installed at the roof of a building to control its dynamic response due to wind or an earthquake. Tuned mass damper consists of a mass, a spring, and a damper anchored or attached to the main structure. During wind or ground excitation, a part of the vibration energy of the main structure is transferred to the TMD system. The TMD parameters (e.g., mass, spring and damping) are typically optimized during the design to have maximum energy dissipated by the TMD system. Generally, TMD is tuned for the

∗Corresponding author, Associate Professor, E-mail: ashutosh.bagchi@concordia.ca
[a] Research Associate, Email:kambiz_esteki@yahoo.com
[b] Professor, Email: sedagha@encs.concordia.ca

Copyright © 2015 Techno-Press, Ltd.
http://www.techno-press.org/?journal=sss&subpage=8 ISSN: 1738-1584 (Print), 1738-1991 (Online)

fundamental frequency of the main structure as the first mode typically has the largest participation in structural response. Thus, TMD which is tuned for the first mode is most effective when the first mode dominates the response. However, the first mode does not always dominate the response of the structure under wide-band excitation frequencies. That could be the case in seismic loading of the structure where multiple modes are significant or in a wind loading which mainly excites the structure in the second frequency and causes the resonance in the second mode of vibration. The traditional passive TMD systems operate in a narrow frequency band and they are basically effective for the vibration frequency for which they are tuned. Therefore, when the difference between the excitation frequency and the tuned frequency increases the TMD system becomes less effective. Several innovative methodologies are available to widen the narrow frequency band of the TMD systems such as designing multiple tuned mass dampers, active tuned mass dampers, hybrid mass dampers and semi-active tuned mass dampers.

Multiple tuned mass dampers consist of several small oscillators with their natural frequencies distributed around the natural frequency of the structure (Jangid 1995, Abe and Fujino 1999). Multiple tuned mass dampers (MTMD) are usually used for vibration control of long-span bridges under critical wind. Active tuned mass dampers (ATMD) are TMD systems collaborating with active control mechanism that can be employed in a structure. In that case, the motion of an auxiliary system is controlled by an actuator to optimize the effectiveness of the TMD system. Hybrid mass damper consists of a small active mass damper (AMD) system attached to a TMD. The TMD is tuned to the fundamental mode of the structure and the AMD improves its effectiveness if vibration includes higher modes of the structure (Cheng *et al.* 2008). On the other hand, a semi-active tuned mass damper (SATMD) is a TMD which is equipped with a semi-active device and associated control system.

The history of using TMD system goes back to 1928 (Ormondroyd and Hartog 1928), while the concept of semi-active tuned mass damper came much later in 1983 (Hrovat *et al.* 1983). Hrovat *et al.* (1983) introduced a semi-active TMD for wind-induced vibrations in high rise buildings. Abe and Igusa (1996) proposed an analytical method for optimal control algorithms of semi-active dampers. Performance of semi-active tuned mass damper in single degree of freedom systems was studied by Aldemir (2003) and Setareh (2001). Chung *et al.* (2005) used a variable damping device and magneto-rheological (MR) fluid damper to show the effectiveness of SATMD. Chey *et al.* (2010) did a comprehensive analytical study on the combination of SATMD and "energy absorbing storey" to mitigate the structural response of a two-story building subjected to earthquake excitation. Pinkaew and Fujino (2001) investigated the control effectiveness of a SATMD with variable damping device under harmonic excitation. Although, LQR and LQG are the most commonly used control algorithm in ATMD and SATMD systems, several other control algorithms were proposed to improve the SATMD performance (Runlin *et al.* 1998, Koo 2003, Liedes 2010, Ghaffarzadeh 2013, Arrigan *et al*. 2014). Ji *et al.* (2005) compared four different control algorithms in SATMD and concluded that among the four control algorithms, DBG (displacement-based ground hook) and clipped optimal algorithm show the best performance under the earthquake loading. Yang *et al.* (2010) also investigated vibration suppression of structures under random base excitation using MR-based SATMD system. They developed an inverse MR-damper model based on an improved version of the LuGre friction model, and then combined with a H2/Linear- H2/LQG controller, in order to control the command current of the MR damper to effectively suppress the levels of structural vibration. Ying *et al.* (2009) studied semi-active stochastic optimal control strategy for nonlinear structural systems with MR dampers. Semi-active control of civil engineering structures with MR dampers attracted a lot of attention

recently (e.g., Yang *et al*. 2002, Jung *et al.* 2004, Amini and Doroudi 2010). The optimum parameters of TMDs that result in significant reduction in the seismic response of structures were the subject of interest in many researches (e.g., Yang *et al*. 2010, Sadek *et al.* 1997, Hoang *et al.* 2008, Rana and Soong 1998, Warburton 1982, Marano and Greco 2010, Sadek *et al.* 1997). Most such research is limited to single degree of freedom systems, while only a few of them considered a wide range of the mass ratio (Esteki *et al*. 2015). In the present research, the response of the structure with passive TMD with a fixed mass ratio has been investigated first. It should be noted that available studies of SATMD to seismic vibration control of buildings are mainly based on laboratory test or model buildings which utilize small MR dampers under harmonic, and limited number of seismic or random excitation. In the present research, a large size MR damper (200 kN) has been implemented to design a SATMD for controlling the seismic response of a high-rise (forty- storey) building for which no reference work is available for comparison. However, the seismic demand of the building with passive and semi-active TMD can be compared to that of the base system without any TMD to estimate the relative performance of a SATMD system. In addition, a simplified model for estimating the dynamic force in a MR damper is proposed to overcome the difficulties associated with the so called phenomenological models in integrating MR dampers to the structural model of a building. The performance of the simplified model of the selected MR damper is compared to a phenomenological model to ascertain its efficacy. The lateral load resisting system of the building considered here consists of typical steel moment-resisting frames designed based on the current versions of the relevant codes and standards in Canada. The response of the structure subjected to a set of seismic ground motions with low, medium and high frequency contents has been calculated to investigate the performance of the building with semi-active tuned mass damper in comparison to that of passive and active TMD systems.

2. Building design

A typical 40-story steel building has been designed according to the provisions of the National Building Code of Canada (NBCC 2010) and the relevant standard (CAN/CSA-S16-09). This building will be used as a benchmark to investigate the effectiveness of the optimally designed semi-active tuned mass system under different seismic excitations. It should be mentioned that TMD is not considered in these stages of design. Once the semi active tuned mass damper and structural design is finalized, the member's sizes in steel moment frames can be refined according to new reduced forces and deformations. The building has nine bays of six meters in one direction and five bays of six meters in another direction and is 122 meters in height as shown in Fig. 1. The lateral load resisting system of building consists of moment resistant steel frames. The dead and live loads are estimated to be 6 kPa and 2.4 kPa, respectively. The seismic and wind load provisions of NBCC (2010) have been applied to estimate the lateral loads. Since the earlier version of the building code NBCC (2005), the equivalent static load-based design procedure is not applicable for buildings higher than 60 m (Yousuf and Bagchi 2010, El Kafrawy *et al.* 2011). In the present case where the building height exceeds the limit of 60 m, the equivalent static load method has been used only for preliminary proportioning of the structural members, while the response spectrum analysis has been used for determining the member forces for the detailed design. The steel structural design has been done using CSA-S16 (2009) standard, and the CISC handbook (2010). The ETABS software (CSI, 2014) has been used for the analysis and design of

the Structure. The columns and beams section used in the building are listed in Table 1.

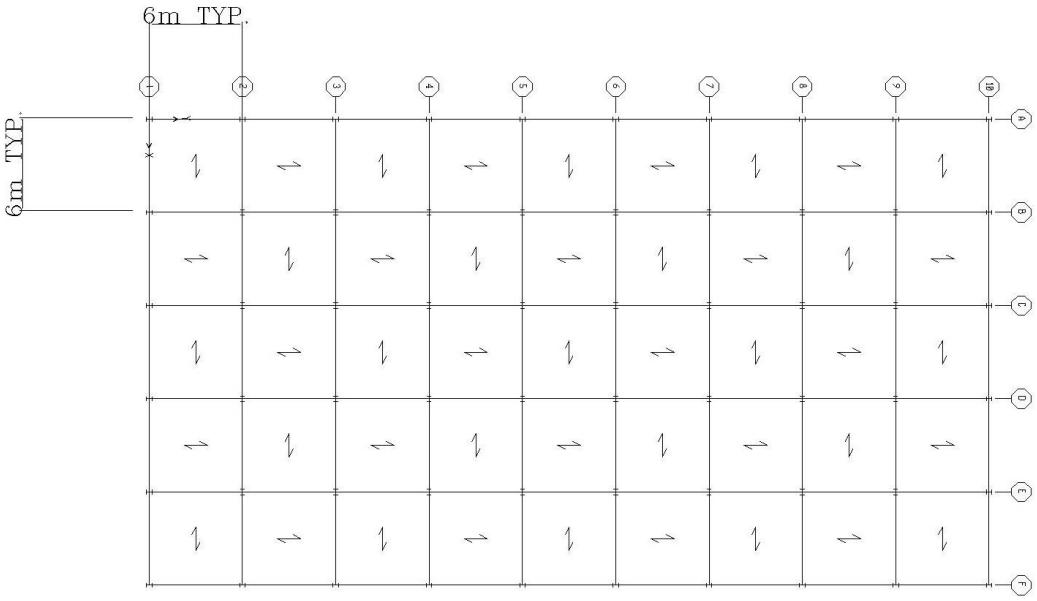

Fig. 1 Beam frame plan and columns layout of 40 story building

Table1 Summary of the column and beam sections

Floor number	Column size	Beam size
1	WWF600x551	W610x101
2-5	WWF500x456	W610x101
6-10	WWF450x409	W610x101
11-15	WWF450x342	W610x101
16-20	WWF400x303	W510x101
21-25	WWF400x243	W610x91
26-30	w610x195	W610x91
31-35	W460x144	W530x82
36-39	W410x114	W460x67
40	Depend on the position of mass(W410x114 mostly)	Depend on the position of mass(W460x67 mostly)

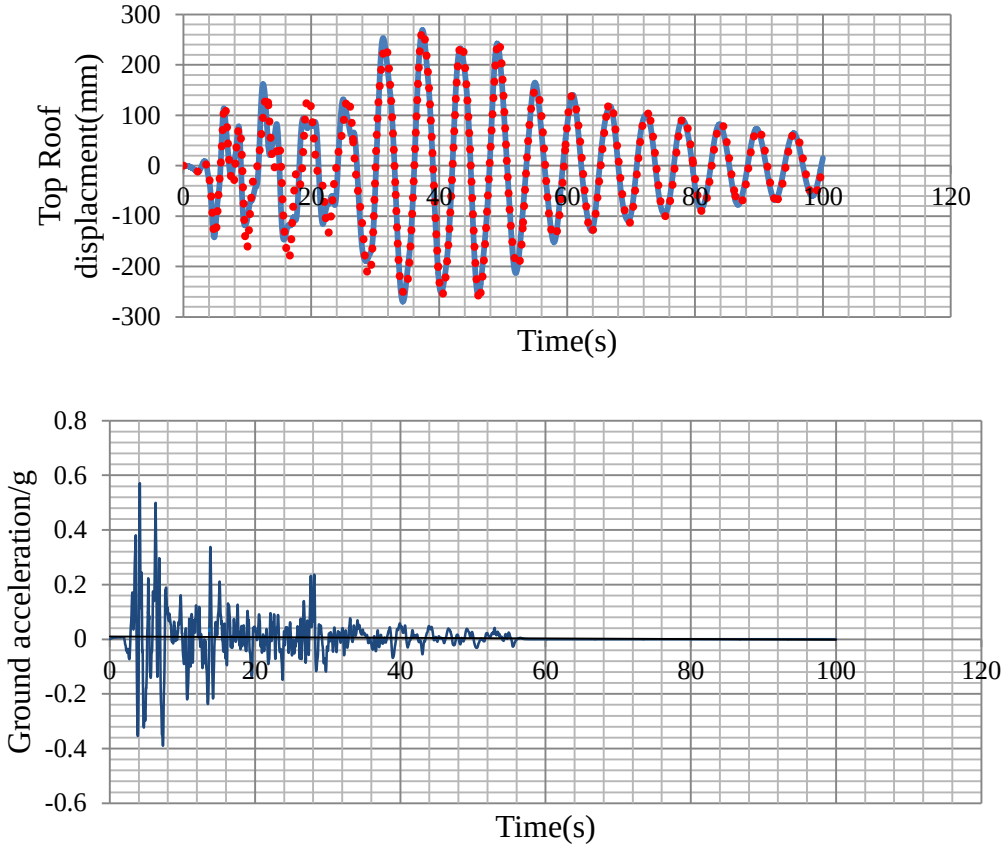

Fig. 2 Bottom: El Centro ground excitation; Top: 3D model in Red (dotted), 2D model in Blue (solid)

3. Finite element model

A three dimension finite element (FE) model of the forty-story building presented in Section 2 has been developed in the ETABS software for the purpose of analysis and design. The FE model has about 7000 degrees of freedom (DOFs) which makes it computationally very expensive for analysis and development of a control system. Thus, the 3D model has been simplified here to an equivalent 2D FE model (shear story building). It should be noted that the simplification has been done in a way that the main DOFs (main floor displacements and velocities) of the system are retained and represented appropriately to the 2D model such that the modal and dynamics characteristics of the 2D and 3D FE models are comparable. Among three main dynamic characteristics of the structure, the mass and damping in the 2D model are kept the same as those in the 3D model. However the stiffness of the 2D model has been altered to achieve the appropriate dynamic responses according to the 3D FE model. While the floor mass and damping properties are kept the same in both the models, structural stiffness matrix in the 2D model has been modified to provide the best agreement between the first mode of vibration of the 3D and 2D

FE models. Then, the dynamic response of the 3D and 2D FE models due to random or seismic loading are compared to justify the modification of the stiffness matrix. The response of top roof floor of the 3D and 2D FE models under El Centro ground excitation has been shown in Fig. 2. The 3D model has been developed using ETABS while 2D model has been implemented in Simulink.

The first four vibration modes of the building are shown in Fig. 3(a).The frequency of these vibration modes and their modal participation factors are given in Table 2. As it can be seen from Fig. 3(a), the torsional vibration modes are excluded from first four vibration modes. First four mode shapes include 94% of modal participation (Table 2). As the building is symmetric, the modal participation of torsional vibration mode is close to zero (Table 3). Thus, eliminating the torsional vibration modes will not introduce any significant error in the calculation, and will simplify the computation very much. The torsional vibration mode shapes are shown in Fig. 3(b).

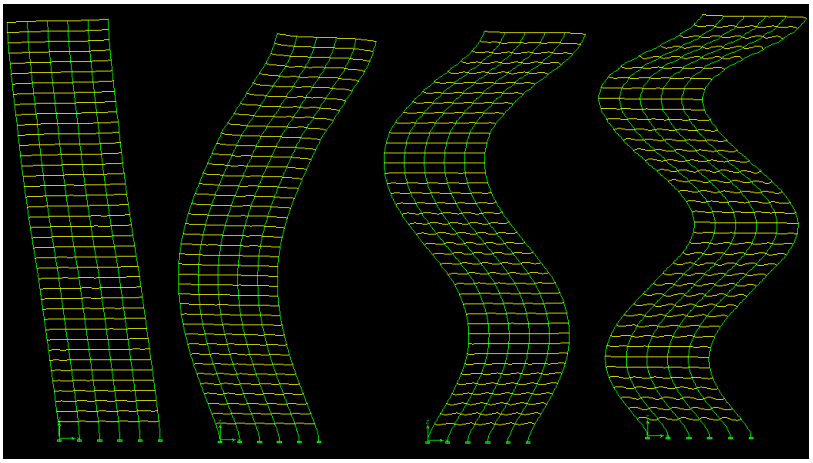

(a)

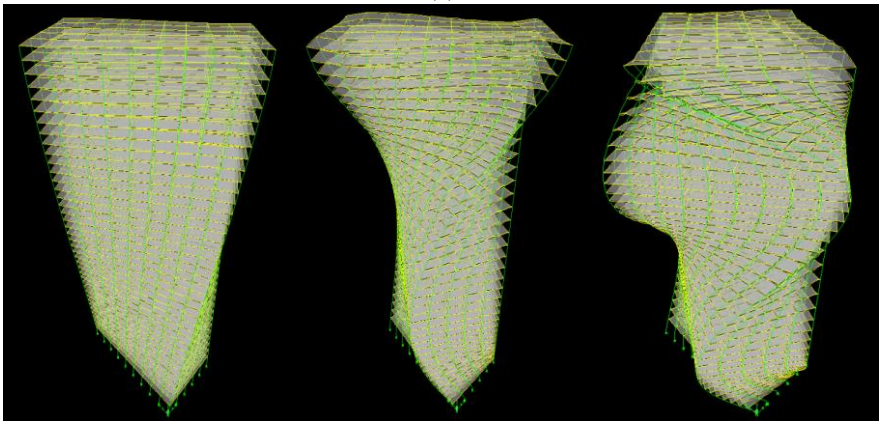

(b)

Fig. 3 (a) Forty Story building mode shapes and (b) Forty story building torsional vibration mode shape

Table 2 Forty story building vibration frequency and modal participation

	First mode	Second mode	Third mode	Forth mode
Period(second)	5.76	2.02	1.22	0.80
Frequency(HZ)	0.18	0.50	0.82	1.24
Modal Participation	75.68	12.82	4.30	2.06
Modal participation summation		94.85 %		

Table 3 The vibration frequency for the torsional modes and corresponding modal participation

	First torsional vibration mode	Second torsional vibration mode	Third torsional vibration mode
Period(second)	4.9	1.8	1.12
Frequency(HZ)	0.2	0.55	0.89
Modal Participation	0	0	0

4. Tuned mass damper (TMD) design

TMD consists of a mass, a spring, and a damper. A simple arrangement of TMD is shown in Fig. 4. The mass is typically limited to the maximum magnitude that can be installed in a structure. A typical TMD and MR damper arrangement is shown in Fig. 5.This arrangement allows the auxiliary mass to move in two perpendicular directions with the help of a rail and frame that are assembled over each other. TMD mass ratio (TMD mass divided by the main structural mass) has a positive direct effect on the structural response and it is recommended that for all practical purposes the mass ratio be mainly limited to about 10 present. For a tall building with height of forty-story such as the one considered in this study, the mass ratio can be between 1.5 to 2 percent (Watakabe *et al.* 2001). Watakabe *et al.* (2001) installed TMD with a mass ratio of 1.73% in a 39-story building. On the other hand, considering the assigned TMD mass ratio, the spring and damping coefficients of TMD system should be carefully designed to provide optimal structural vibration suppression. Here, the stiffness and damping of the TMD system have been altered from 20% to 200% of the values corresponding to the perfect tuning condition and the response of the structure during ground motion has been determined accordingly. Although this approach provides a pair values for the stiffness and damping of an optimal TMD system (based on minimum displacement), it is observed that different ground motion needs different pair of optimal stiffness and damping ratio for the TMD system.

The pilot structure used in this research (i.e., the 40 story building) has been investigated using different ground motions. In case of perfect tuning, the natural frequency of a TMD should be

equal to the fundamental frequency of the main structure. For the mass ratio of 1.5%, perfect tuning requires that:

$$m_{TMD} = 0.015 \times M_{structure}$$
$$\omega_{TMD} = \omega_{struture} \tag{1}$$

Thus

$$\frac{k_{TMD}}{m_{TMD}} = \omega^2{}_{struture} \quad ; \quad c_{TMD} = 2 \times \xi_{structure} \times m_{TMD} \times \omega_{struture} \tag{2}$$

5. Control algorithms

Equations of the motion of seismically excited structure in the finite element form can be expressed as (Ogata 2010)

$$M_S \ddot{Z} + C_S \dot{Z} + K_S Z = \Lambda U - M_S \Gamma \ddot{x}_g \tag{3}$$

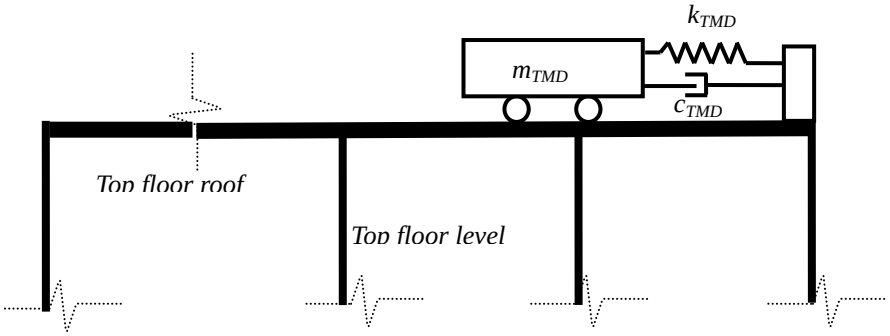

Fig. 4 Typical arrangement of TMD system

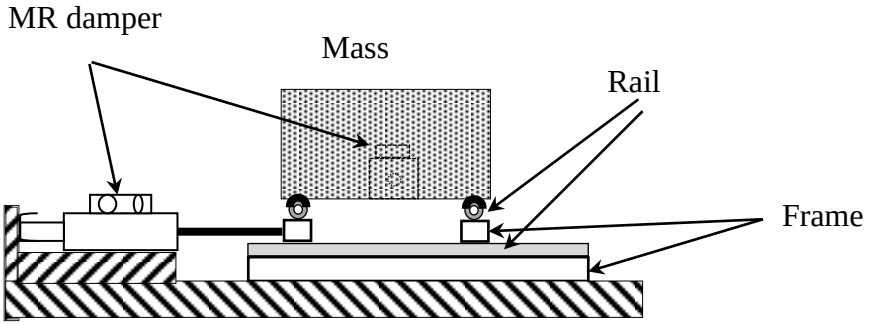

Fig. 5 Typical arrangement of connection between the TMD and the MR damper

Where, M_s, C_s and K_s are the mass, damping and stiffness matrices of the system. U is the control force vector, Λ is the control force location matrix, and Γ is the direction matrix related to the base acceleration, $\ddot{x}_g$.

The equations of the motion as given by Eq. (3) are transformed into a state space representation (also known as the "time-domain approach") to provide a convenient way to model and control a system with multiple inputs and outputs. To accomplish this, one may write

$$\begin{cases} x_1 = z \\ x_2 = \dot{z} \end{cases} \tag{4}$$

Where the first state x_1 is the displacement and the second state x_2 is the velocity. Using the above change of variables, the state space presentation of Eq. (3) can be written as

$$\dot{X} = AX + BU + E\ddot{x}_g \tag{5}$$

Where A, B, C, D are matrices defined as

$$A = \begin{bmatrix} 0 & I \\ -M_S^{-1}K_S & -M_S^{-1}C_S \end{bmatrix} \tag{6}$$

$$C = \begin{bmatrix} -M_S^{-1}K_S & -M_S^{-1}C_S \end{bmatrix} \tag{7}$$

$$B = \begin{bmatrix} 0 \\ -M_S^{-1}\Lambda \end{bmatrix} \tag{8}$$

$$E = \begin{bmatrix} 0 \\ \Gamma \end{bmatrix} \tag{9}$$

$$D = \begin{bmatrix} -M_S^{-1}\Lambda \end{bmatrix} \tag{10}$$

And $X=\{x_1, x_2\}$ is the state vector

As it can be seen from Eq. (5), the state vector (X) is related to its derivative in time domain, control force (U) and ground excitation. State space model of a structure under seismic excitation and control forces can be solved using the relevant numerical tools such as those available in MATLAB/SIMULINK (Mathworks 2011a,b). The theory of optimal control is concerned with operating a dynamic system at the minimum cost. If the system dynamics is represented in the form of linear differential equations and the cost function can be written as a quadratic function, the LQR control strategy can be used to minimize the cost function. For the structural system, cost function can be written as

$$J = \int_0^t (X^T QX + U^T RU)dt \tag{11}$$

The first term in Eq. (11) represents the structural kinetic energy due to vibration and second term represents work done by the control force. Q and R are arbitrary positive semi-definite and

positive definite matrices, respectively which are used to tune the control system. For example, if the *Q* matrix has small components, it results in large displacements and velocity in the system. On the other hand, if the elements of *Q* matrix have large values, it results in small displacements and velocity, but large gain factor (control force) which may not be practical. Also large values in the *R* matrix would cause small gain (small control force) and large displacements, while small values would produce large gain (large control force) and small displacements. It should be noted that *Q* and *R* matrices should be chosen in such a way that the gain matrix satisfies the maximum allowable displacements and maximum applicable control forces. The control gain matrix *K* can be written as

$$K = R^{-1}B^{T}P \tag{12}$$

where, *P* is the Riccati matrix which is governed by the following equation called Riccati equation:

$$-\dot{P}(t) = A^{T}P(t) + P(t)A + R - P(t)BR^{-1}B^{T}P \tag{13}$$

The solution of the LQR problem (control force) can now be written as

$$U = -KX \tag{14}$$

Fig. 7 shows a block diagram of the state space representation of equations of motion. The vector of states (*X*) is multiplied by matrix *A* to give dynamic forces of the structure. In addition vector of states (*X*) is used to compute control forces by multiplying the gain matrix (*K*) by it (U=-K*X). Computationally speaking, this procedure considers ground excitation as the input signal and tries to minimize the response of the system by introducing the control force into the system (structure).This control force (in this case, the force in TMD) is limited to the capacity of the actuators or that of the semi-active damper (e.g., MR damper).

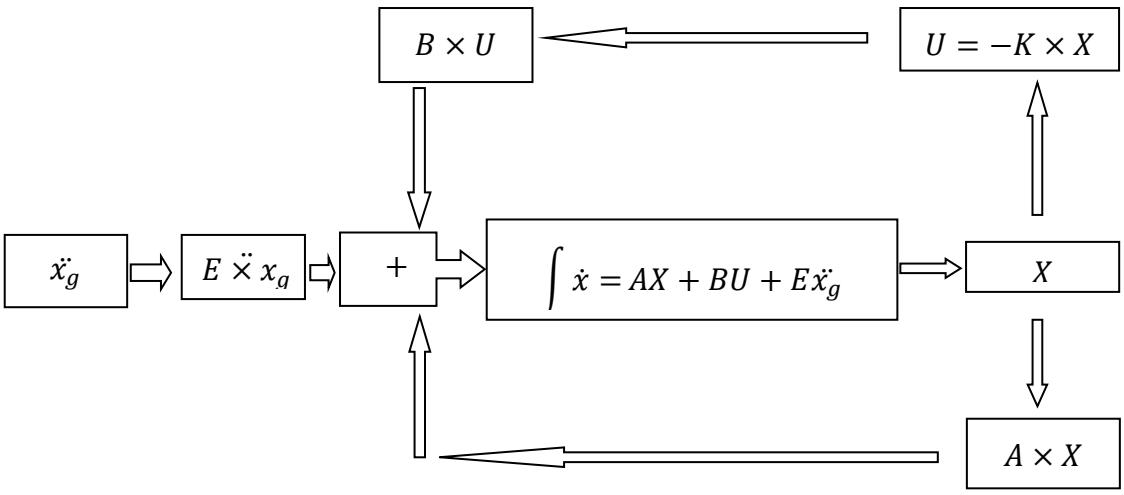

Fig. 7 State space flow chart for SATMD and TMD analysis

The control force obtained from Eq. (14) should be augmented by a semi-active control strategy in order to be used with a semi-active control system. A semi-active control system with an MR damper can only apply passive force, F_{MR} which is opposite to the direction of the relative velocity of the two ends of the MR damper, v_{rel}, an their relationship can be expressed as

$$F_{MR} \propto -sign(v_{rel}) \tag{15}$$

This applicable passive force, F_{MR} is only useful when it has the same direction as the calculated active control force, U as given by Eq. (14). If F_{MR} has the opposite direction as compared to U, it should not be applied. Thus, the semi-active control strategy can be described as

$$\begin{cases} if \quad U \times F_{MR} \geq 0 & Apply \;\; I_{\max} \\ if \quad U \times F_{MR} \leq 0 & Apply \;\; I = 0 \end{cases} \tag{16}$$

where, I and $I_{\max}$ denote the electrical current and the maximum electrical current which is applicable to a specific MR damper.

6. The semi-active tuned mass damper

One type of semi-active control device is magneto-rheological (MR) fluid damper. The MR fluid is very sensitive to the applied magnetic field and changes from liquid to semi–solid material in millisecond. This unique feature enables to build a variable damping device with MR fluid (MR damper) with minimal power requirements.

In this study, a 200 kN (20 ton) MR damper similar to that studied by Yang *et al.* (2002) has been utilized in the semi-active tuned mass damper (SATMD). If one damper is not adequate, one may use multiple SATMD dampers to generate the adequate damping force. One restriction that cannot be generally satisfied in the design process of SATMD is the damper stroke length. The 200 KN MR damper has 8 cm stroke length, however practically the stroke of 40 cm is required (Watakabe *et al.* 2001).To continue with research, It is decided to use the MR damper with 40 cm stroke, while limiting the damper force to 200 KN.

The 20 ton MR damper can be modeled using the modified Bouc-Wen model as reported in Yang *et al.* (2002), while the input signal is low pass filtered. This filtering helps the numerical procedure to be stable but generates error when control algorithms use this input to provide commands to MR damper, especially when cutting frequency is as low as 5 Hz. In the current research, a simple phenomelogical model has been developed for a 20 ton MR damper based on the Mechanistic models of MR/ER dampers developed by the authors earlier (Esteki *et al.* 2011, 2014). In this model, the damping force in the MR device is related to the strut velocity and the current which governs the yield stress of the MR fluid. The model can very well approximate MR damper force in random vibration. The maximum useful current for MR damper which is used in this study and also used by Yang *et al.* (2002) is 1 Amp. This current is chosen from design chart provided by the manufacturer. Under constant current of 1 Amp, the damping force can be simply expressed as

$$F_D = 1.95 \times 62 \times 10^3 \times sign(v) + 13.15 \times sign(v) \times v^2 \tag{17}$$

If the current is zero

$$F_D = 0.4526 \times 62 \times 10^3 \times sign(v) + 5.7904 \times sign(v) \times v^2 \quad (18)$$

where v is in (mm/s) and F_d in (Newton).

The damping force estimated by the proposed model has been verified for the above two cases with that obtained using the modified Bouc-Wen model as given in Yang *et al.* (2002). Sample results are shown in Figs. 8 and 9 under constant current of one or zero Ampere. Generally, there is a very good agreement between the results obtained from the proposed simplified model and that from the Bouc-Wen model. As the Bouc-Wen model is iterative and computationally intensive, it is difficult to integrate to a structural analysis system of a multistory building involving a large system of equations. The simplified model is very fast and can be easily integrated to the structural model of a building. This is particularly advantageous when a building employing MR dampers needs to be analyzed for a suite of multiple ground motions to assess the seismic performance of the building.

7. Analyses of the 40-story building equipped with SATMD

In current research the performance of 40-story tall, steel structure equipped with semi-active tuned mass damper or SATMD has been studied. To better realize the characteristics and functionality of the SATMD system designed here, the analysis of the structure has been carried out for six different earthquake ground motion records selected from the database maintained by the Pacific Earthquake Engineering Research Center (PEER) at the University of California Berkeley. The selected ground motion records contain low, medium or high frequency contents; and the details of the records are given in Table 4.

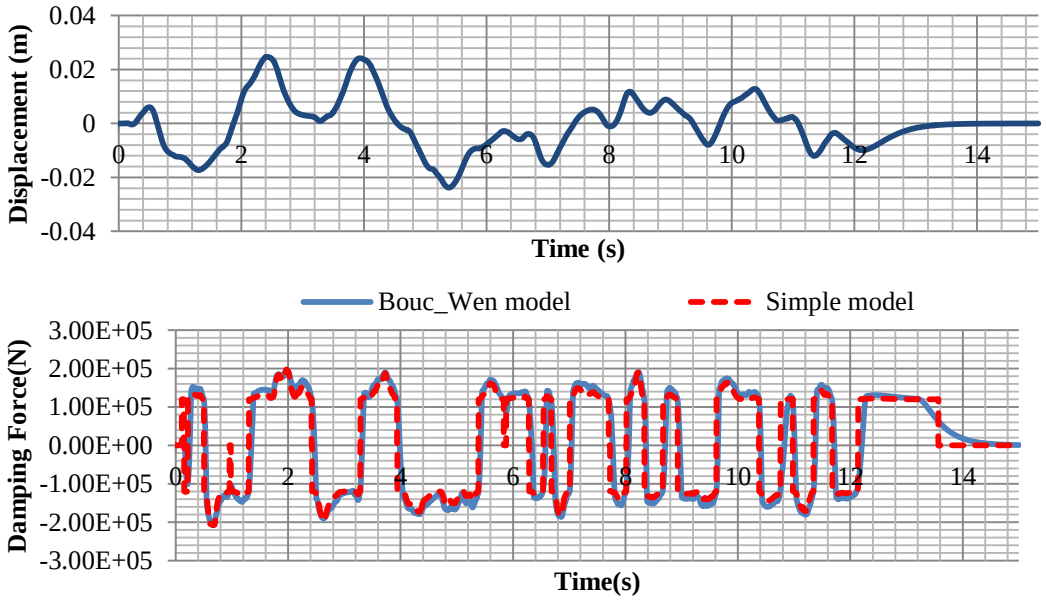

Fig. 8 Random excitation (top) and MR damper force (bottom) at constant current of i = 1 Amp

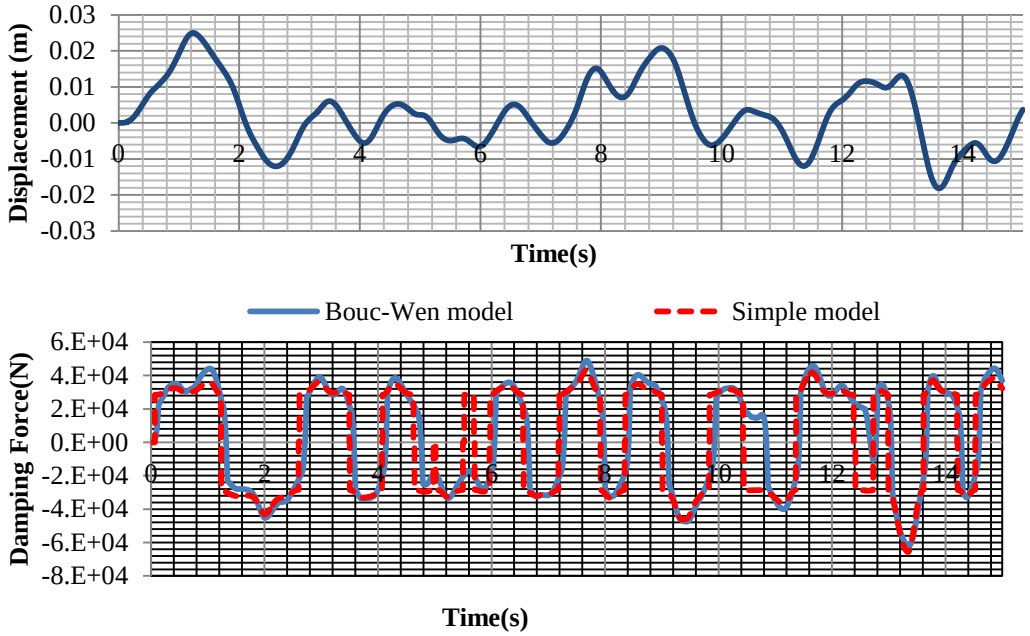

Fig. 9 Random excitation (top) and MR damper force (bottom) at constant current of i = 0 Amp

Table 4 The details of the ground motion records used in the analysis

Ground motion name	Location	Year	Category (low, medium and high frequency content)
Kobe	Japan	1995	low
Irpinia	Italy	1980	low
Kocaeli	Turkey	1980	low
Tabas	Iran	1978	Medium to high
Nahanni	Canada	1985	Medium to high
Upland	California	1990	Medium to high

The results are shown in time domain as well as frequency domain. All earthquake records are scaled to 0.2 g to represent in the seismicity of Vancouver, Canada where the building being studied is assumed to be located. Kobe ground acceleration record and its Fast Fourier Transform are shown in Fig. 10. Kobe ground acceleration record has duration of about 20 seconds and its FFT analysis shows frequency contents to be in the range of 1 to 5 Hz. The roof displacement of the structure due to the scaled Kobe ground acceleration is shown in Fig. 11. As it can be seen from the figure, while both TMD and SATMD reduce the response of the structure for up to 20

seconds, SATMD performs better than the passive TMD. After 20 seconds, SATMD shows its superior performance by suppressing the vibration completely, while passive TMD system does not damp out the vibration that effectively.

The performance of TMD and SATMD can be better studied in the frequency domain. Fig. 12 shows the comparison of the frequency response of the uncontrolled structure with those of controlled structures using passive TMD and SATMD systems. It can be observed that, TMD decreases the first vibration mode appreciably; however it generates other two peaks in right and left side of fundamental frequency.

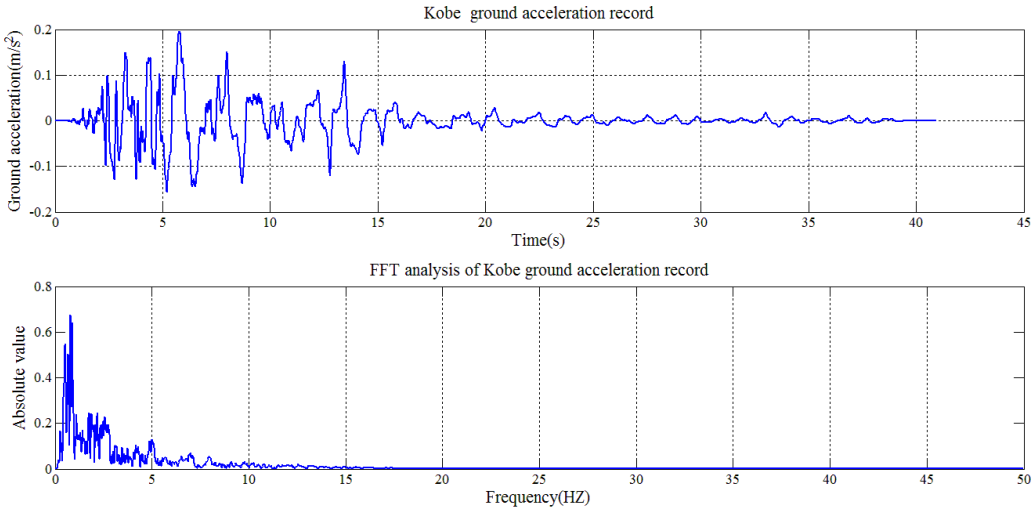

Fig. 10 Kobe ground acceleration record and its FFT diagram

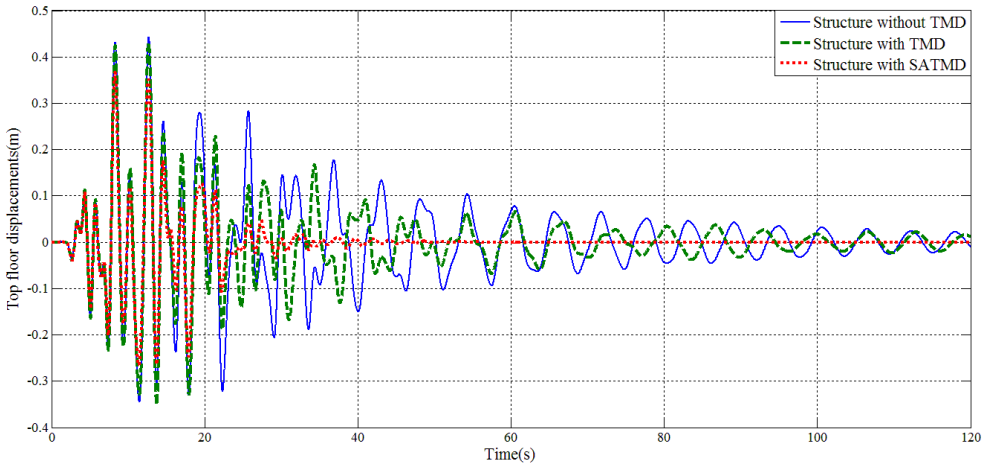

Fig. 11 Roof displacement of the structure due to Kobe ground motion in time domain

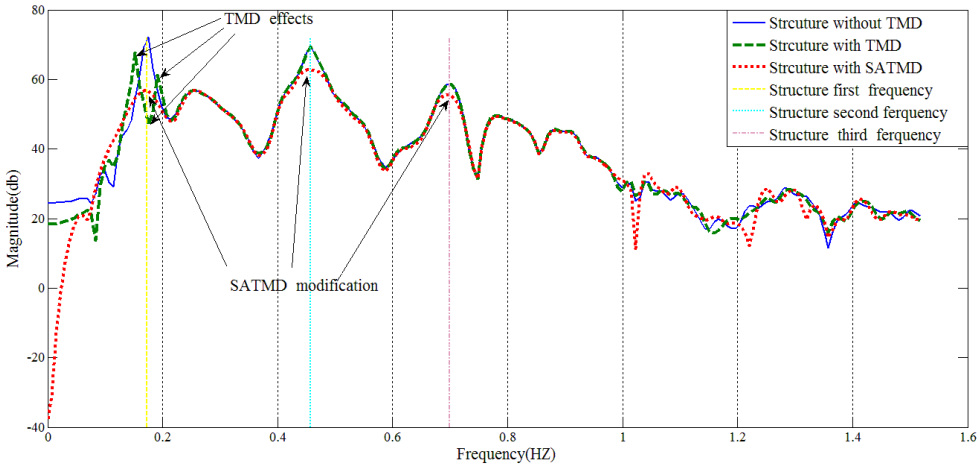

Fig. 12 Roof displacement of the structure due to Kobe ground motion in frequency domain

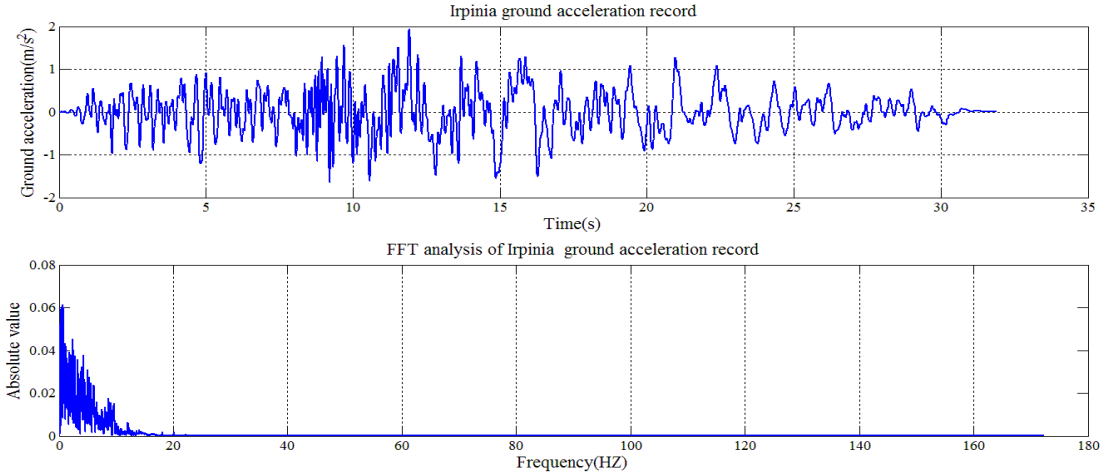

Fig. 13 Irpinia ground acceleration record and its FFT diagram

SATMD generally performs better in the given frequency range and clearly suppress the vibration in the above mentioned two peaks generated by passive TMD. In addition. it can be seen from Fig. 12 that SATMD not only reduces the response at the first mode frequency but also reduces the frequency responces at higher modes such as the second and third modes. This means that SATMD increases the effectiveness of TMD for the second and third modes of vibration; or in the other words, it expands the frequency band of a TMD system. The same conclusion can be deduced for Irpinia (Figs.13-15) and Kocaeli earthquake records as observed in Figs. 16-18. The maximum diplacment reduction in roof displacement and settling time for three seismic records with low frequency contents is provided in Table 5. The seismic records with low frequency contents are choosen since they induce a large deformation in tall structure because of their low frequency contents would be closer to the natural frequency of the structure.

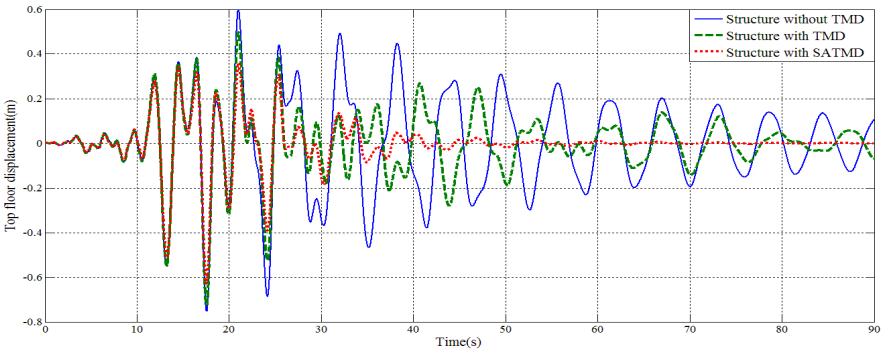

Fig. 14 Roof displacement of the structure due to Irpinia ground motion in time domain

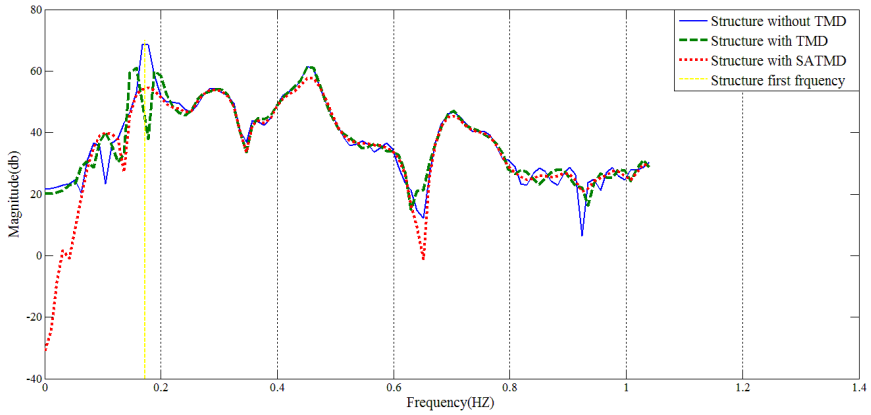

Fig. 15 Roof displacement of the structure due to Irpinia ground motion in frequency domain; TMD effect

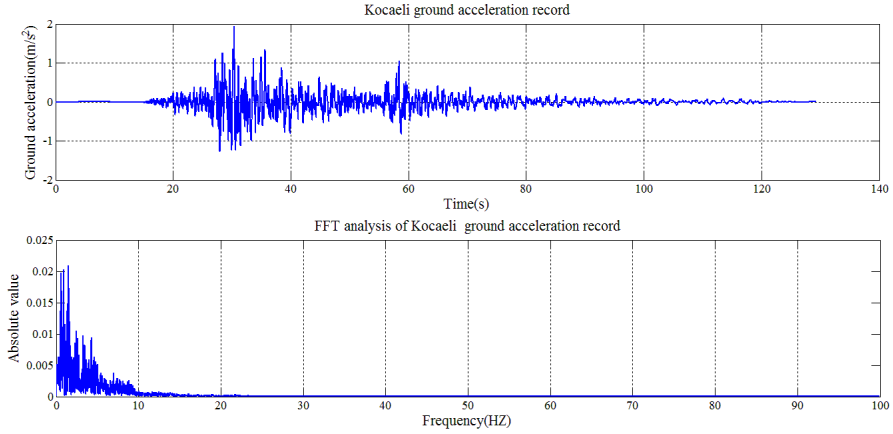

Fig. 16 Kocaeli ground acceleration record and its FFT diagram

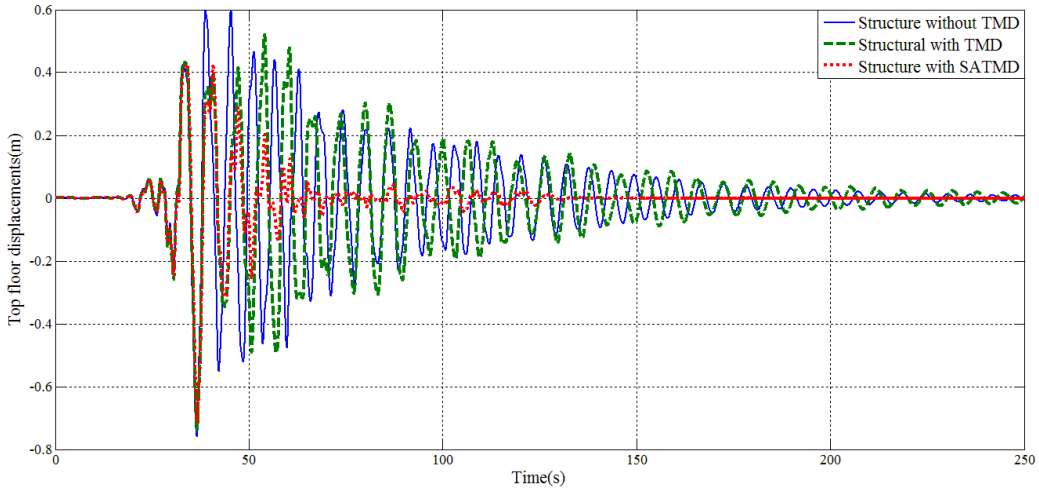

Fig. 17 Roof displacement of the structure due to Kocaeli ground motion in time domain

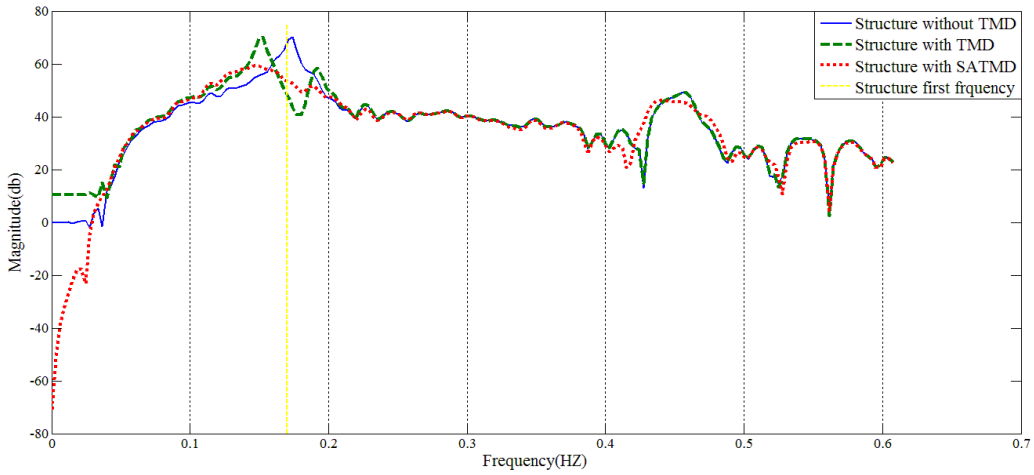

Fig. 18 Roof displacement of the structure due to Kocaeli ground motion in frequency domain; TMD effect

Table 5 clearly shows the superior performance of SATMD system as compared to a conventional TMD system. As it can be seen from Table 5, the SATMD reduces maximum displacements more effectively than the conventional TMD system, and the main advantage of the SATMD is observed in the reduction of the setting time which is almost less than half of that of TMD.

The behavior of TMD and SATMD in the cases of earthquake records with medium and high frequency contents (including Tabas, Nahanni and Upland) is also investigated. The response of the building to these earthquakes is shown in Figs. 20 to 27. The time histories and the frequency

contents of these earthquake records are shown in Figs. 17, 20 and 23. Since the distribution of frequency of these seismic records do not match the fundamental frequency of the structure, they cause very small deformation. The roof displacement is about 150 mm due to the Tabas ground motion record; and 60 mm and 10 mm due to Nahanni and Upland records, respectively. These displacements for a tall building which is 120 m high are quite negligible. Similar levels of improvement in the response of the structure is found when it is equipped with SATMD as compared to passive TMD, both in time domain (Figs. 20, 23 and 26) and frequency domain (Figs. 21, 24 and 27). The maximum reduction in displacements and settling time for the seismic records with medium and high frequency ranges in the 40 story building with TMD and SATMD are shown in Table 6.

Table 5 Reduction in the maximum displacements, and settling time for low frequency seismic records

Ground motion record	Maximum reduction in the peak displacements (percent)		Settling time (s)	
	TMD	SATMD	TMD	SATMD
Kobe	2.5	17	67	27
Irpinia	3.8	16.5	90	34
Kocaeli	2.9	6	159	64

Table 6 Reduction the maximum displacements, and settling time for the ground motion records medium and high frequency ranges

	Maximum reduction in displacements (%)		Settling time (s)	
	TMD	SATMD	TMD	SATMD
Tabas	6	11	70	30
Nahanni	21	27	35	15

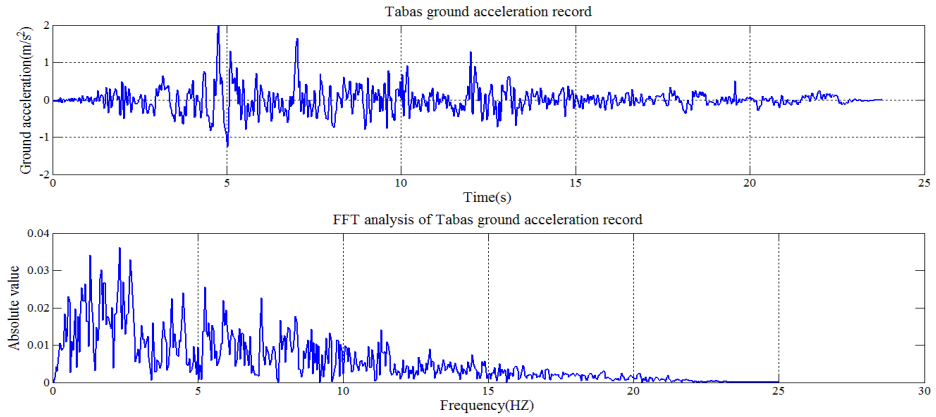

Fig. 19 Tabas ground acceleration record and its FFT diagram

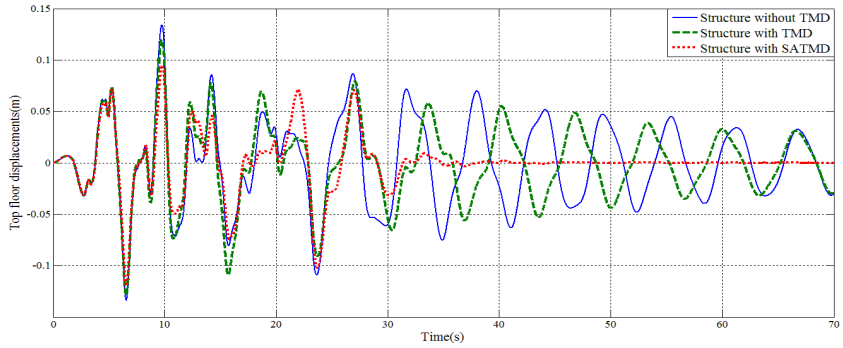

Fig. 20 Roof displacement of the structure due to Tabas ground motion in time domain

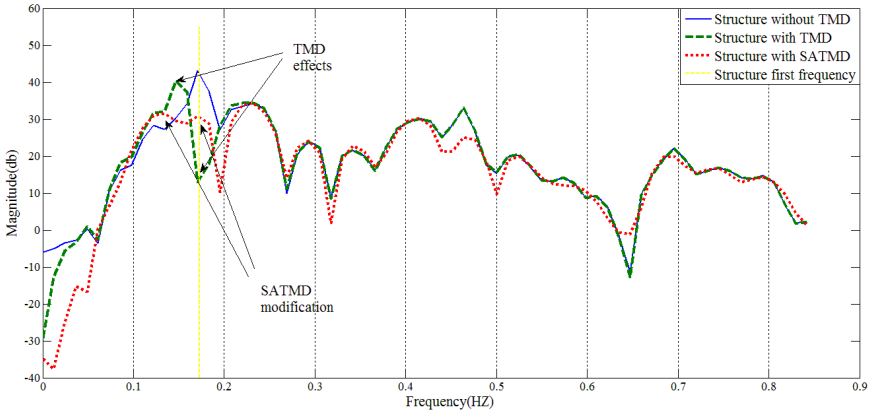

Fig. 21 Roof displacement of the structure due to Tabas ground motion in frequency domain

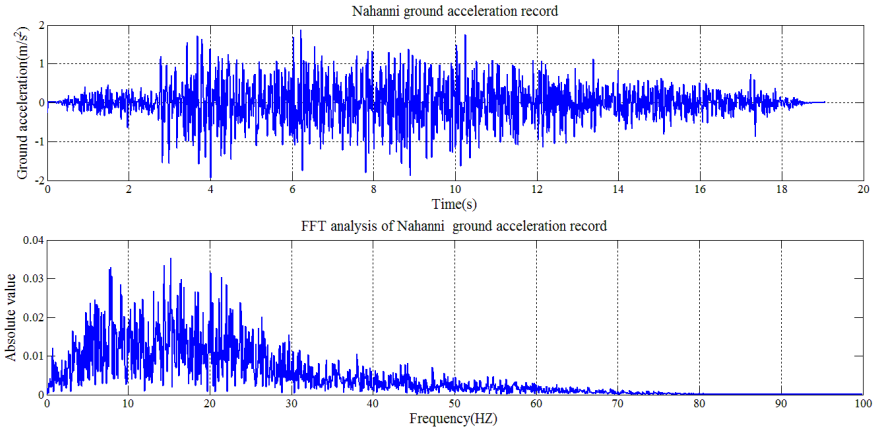

Fig. 22 Nahanni ground acceleration record and its FFT diagram

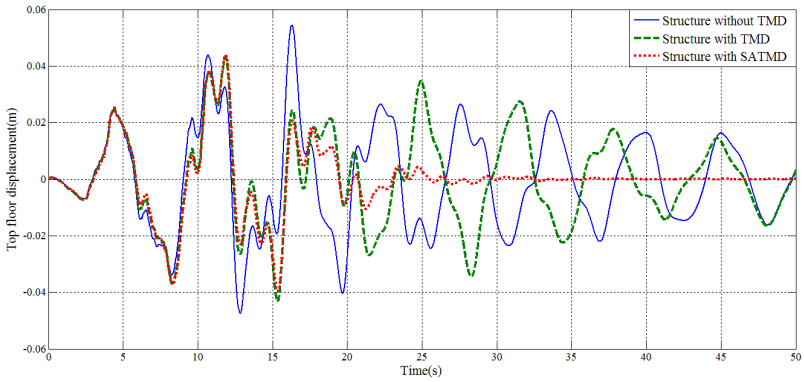

Fig. 23 Roof displacement of the structure due to Nahanni ground motion in time domain

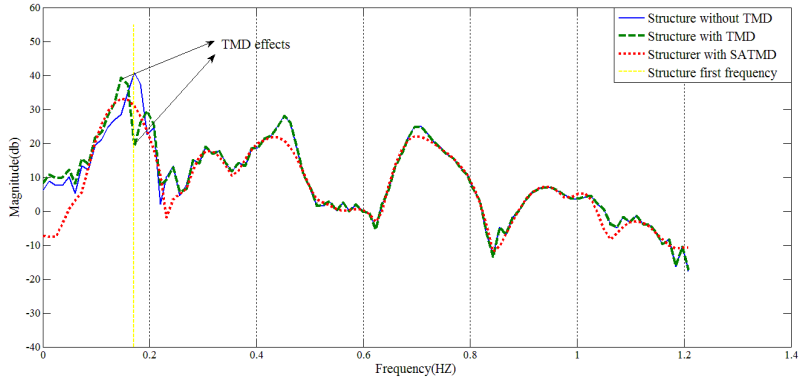

Fig. 24 Roof displacement of the structure due to Nahanni ground motion in frequency domain

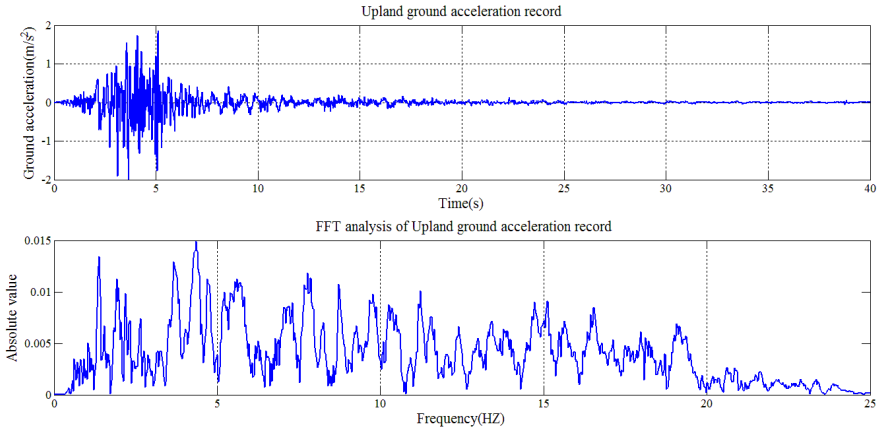

Fig. 25 Upland ground acceleration record and its FFT diagram

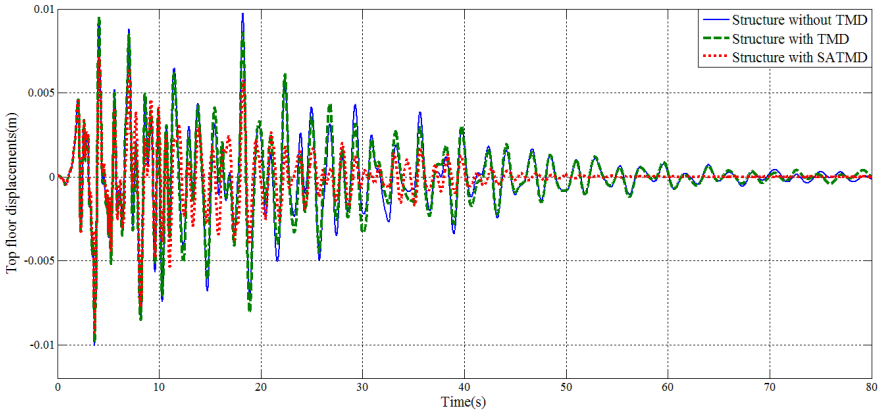

Fig. 26 Roof displacement of the structure due to Upland ground motion in time domain

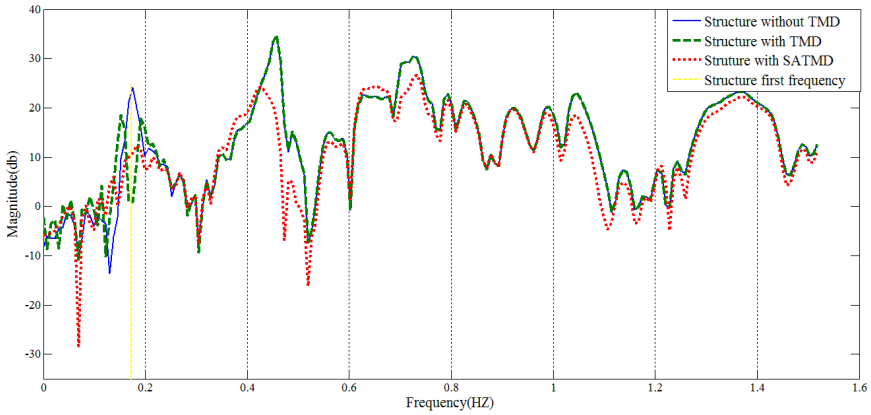

Fig. 27 Roof displacement of the structure due to Upland ground motion in frequency domain

8. Tuning of the control system

The performance of control system directly affects the response of SATMD system. LQR control algorithm uses optimization to determine the gain matrix in order to optimize the cost function. Thus, defining various cost functions will results in different gain matrices and different control forces, and consequently different structural responses. The cost function, J, in Eq. (11) is a combination of the state vector (displacements and velocities) and the control force vector weighted by the coefficients defined by Q and R matrices, respectively. Therefore, Q and R matrices can change the cost function, gain matrix, control force, and the structural response, as explained in Section 5. R is a unit matrix multiplied by a constant coefficient which should be determined so that the gain matrix can yield applicable control forces. In the current research, the response of the structure with SATMD system using three different Q matrices has been

investigated. Q_1 (Eq. (19)) considers both displacement and velocity, Q_2 (Eq. (20)) considers only velocity, and Q_3 (Eq. (21)) considers only displacement.

In using Q3 in Eq. (11), the structural displacements will be included in the cost function and the object of the control system is to minimize the structural displacements (except TMD mass displacement). On the other hand, if matrix Q1 and Q2 are used, the control system will minimize both structural displacements and velocity. The response of the structure has been computed using Q1, Q2 and Q3, and illustrated in Fig. 26.

$$Q_1 = \begin{bmatrix} 1_{41\times41} & 0_{41\times41} \\ 0_{41\times41} & 1_{41\times41} \end{bmatrix} \tag{19}$$

$$Q_2 = \begin{bmatrix} 0_{41\times41} & 0_{41\times41} \\ 0_{41\times41} & 1_{41\times41} \end{bmatrix} \tag{20}$$

$$Q_3 = \begin{bmatrix} 1_{41\times41} & 0_{41\times41} \\ 0_{41\times41} & 0_{41\times41} \end{bmatrix} \tag{21}$$

As it can be seen from Fig. 28, the variation of Q matrix greatly alters the results of the SATMD system. The best results for minimizing the top floor displacement is reached by Q matrix defined in Eq. (21). Eq. (21) results in a cost function which contains the structural displacements only.

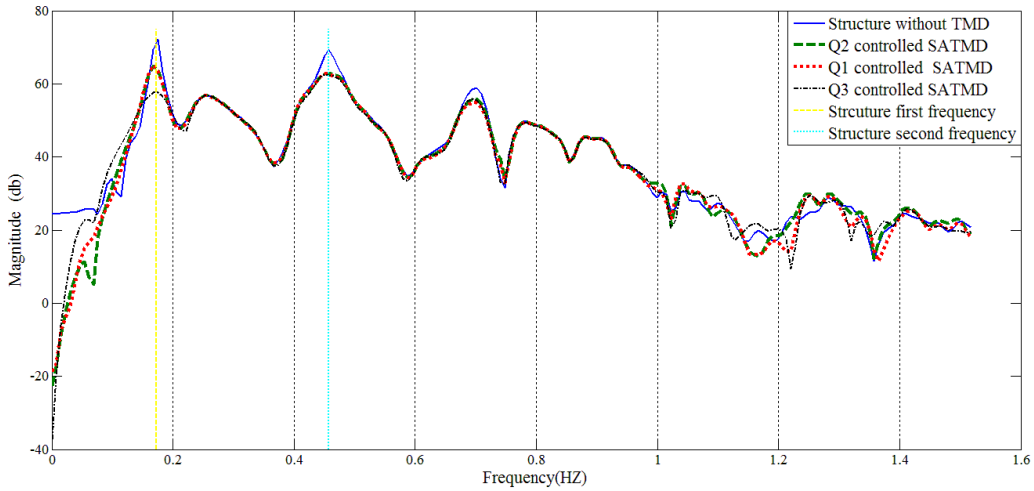

Fig. 28 Roof displacement of the structure with different Q weighting matrix due to Kobe ground motion in frequency domain

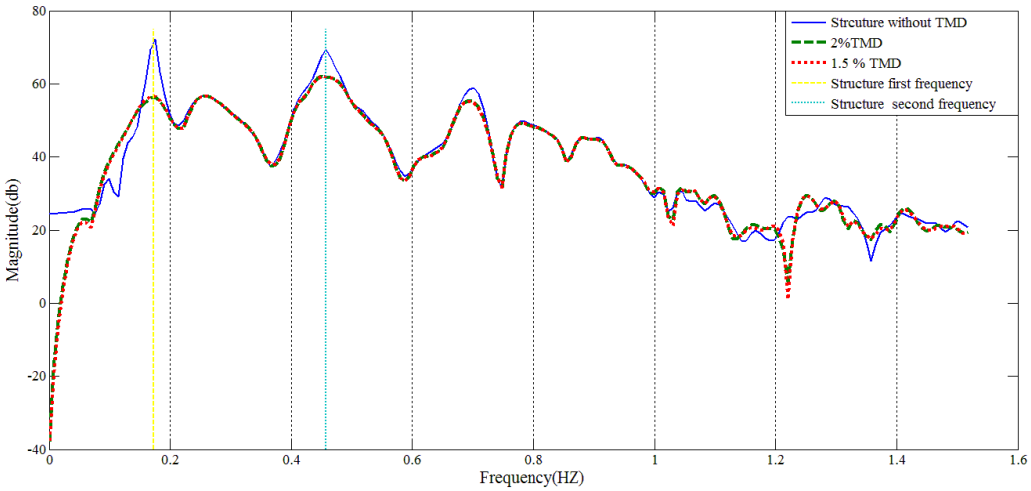

Fig. 29 Roof displacement of structure with different mass ratio for SATMD due to Kobe ground motion in frequency domain

9. Mass ratio effect on response of SATMD system

The influence of the mass ratio (i.e. the mass of the TMD divided by the mass of the structure) on the response of the tall building with SATMD system subjected to Kobe earthquake excitation is illustrated in Fig. 29. In low rise building or light weight mechanical systems the mass ratio can be increased up to 10 percent. For high rise buildings and heavy mechanical systems mass ratio is is kept low. In Fig. 27, the mass ratio is increased from 1.5 percent to 2 percent which is within a practical range of mass ratio for a 40-story tall building. As it can be realized, the increase of mass ratio from 1.5 percent to 2 percent has little to no effect on the response of the structure. It is noted that the difference in the response of the structure due to the change in the mass ratio is not visible in the time domain. For that reason, only frequency domain response is reported in Fig. 29. Thus the results suggest that increasing mass ratio in SATMD system in the practical range of 0.5% to 1 % will not improve the efficiency of SATMD system.

10. Semi-active versus active tuned mass damper

Although, SATMD system decreases the magnitude and duration of structural vibration very effectively, it does not reduce the maximum displacement in some cases. To explain this disadvantage, tall structures with different TMD systems (including active tuned mass damper) are considered to explain the differences. The structure with an Active TMD (ATMD) system is subjected to the Kobe earthquake motion and the same LQR control algorithm as the semi-active control system has been used. The maximum actuator force is assumed to be 5000 kN which is about six times the force needed in SATMD. The only disadvantages of ATMD is that this 5000 kN should be generated by actuators while 800 kN damping force in SATMD can be produced by

changing the magnetic field around the MR fluid for which the power can be supplied by a battery. The results for top floor displacement are shown in Figs. 30 and 31. As it can be observed, an ideal ATMD not only decreases the magnitude and the duration of the structural vibration, but also, considerably reduces the maximum displacements of the structure. This reduction in the maximum displacements by ATMD is achieved by pulling and pushing of the auxiliary mass in appropriate directions which cannot be performed in SATMD.

An ideal ATMD is expected to decreases the peak displacements in a high-rise building to as much as 40%. However, it should be noted that in real engineering practice, active control system is limited to applicable gain or specifically to the power of the electrical machine that will produce the forces to pull or push the mass of TMD system. The power requirement for an actuator in ATMD system to produce such a large force is quite high, and since at the time of an earthquake power failure is more likely, the ATMD system may not remain operational. For that reason, an SATMD system is preferable as the power requirement is low and the system can remain operational even in the case of a power failure as the power can be supplied to the SATMD system by a battery.

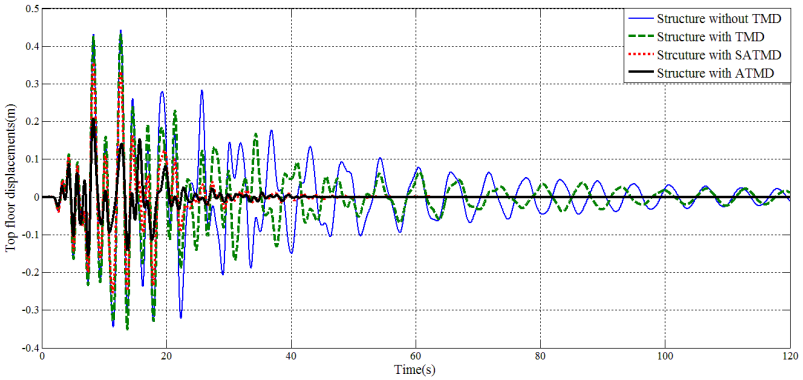

Fig. 30 Roof displacement of the structure due to Kobe ground motion in time domain (ATMD)

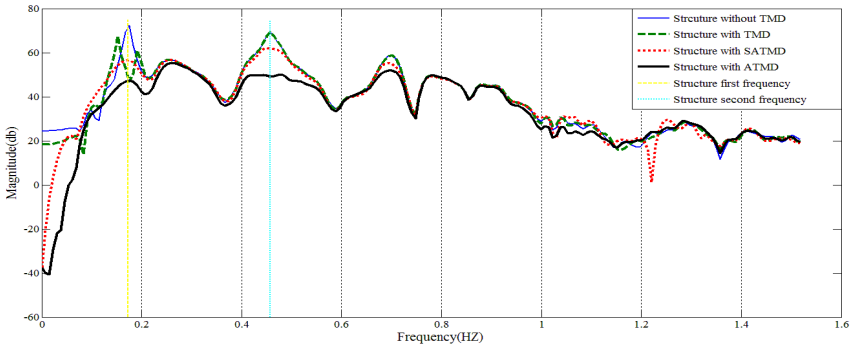

Fig. 31 Roof displacement of the structure due to Kobe ground motion in frequency domain (ATMD)

11. Conclusions

In this paper a MR-based semi-active tuned mass damper system (SATMD) has been designed to control the vibration of a 40-story tall building with steel moment resisting frames designed according to the National Building Code of Canada (NBCC 2010) and the relevant standard for steel design (CAN/CSA-S16-09). A simplified model for calculating the damping force in the selected MR flud damper of 200 kN capacity has been proposed and its performance is found to be comparable to the modified Bouc-Wen model. The simplified model of the MR damper is easy to integrate to the structural model of the building in order to carry out the seismic response history analysis using a suite of earthquake ground motion records.

For MR fluid-based semi-active control of TMD, the LQR control algorithm has been used to find the optimal damping forces. The seismic response of the uncontrolled structure and controlled structure equipped with traditional passive TMD system and SATMD system under different earthquake records with low, medium and high frequency contents have been determined and compared. It has been shown that SATMD system has superior performance as compared to the traditional TMD system in reducing the displacement demand as well as the settling time of the structure. SATMD system can suppress the vibration in a wide range of frequencies in contrast to TMD system which is tuned at a particular frequency.

To minimize the structural response due to a seismic excitation, an optimal Q matrix for LQR control system in TMD application has been proposed. Furthermore, it has been illustrated that in a practical range of the auxiliary mass in a tall building (1.5% to 2.5% of building mass), the response of structure does not change appreciably.

Finally, it has been shown that in spite of the obvious advantages of a semi-active control system versus the passive control system in reducing the seismic response of tall structures, the active control system is the most effective one for a TMD system provided the power requirements are met for the actuator to produce a large push and pull forces, in case of an earthquake. In the event of a power failure during an earthquake an active system will fail to operate unless there is a backup power supply. Also, and active system has a potential for instability when the actuator force is applied iappropriately. On the other hand, SATMD may remain operational even in the case of a power failure during an earthquake and provide effective vibration control to a structural system. Since there is no actuation involved with SATMD, the system is stable even when the control system develops any problem.

Acknowledgments

The support of the Natural Sciences and Engineering Research Council of Canada (NSERC) is gratefully acknowledged.

References

Abe, M. and Fujino, Y. (1999), "Dynamic characterization of multiple tuned mass dampers and some design formulas", *Earthq. Eng. Struct. D.*, **23**(8), 813-835.

Abe, M. and Igusa, T. (1996), "Semi-active dynamic vibration absorbers for controlling transient response", *J. Sound Vib.*, **198**(5), 547-569.

Aldemir, U. (2003), "Optimal control of structures with semi-active tuned mass dampers", *J. Sound Vib.*, **266(**4), 847-874.
Amini, F. and Doroudi, R. (2010), "Control of a building complex with magneto-rheological dampers and tuned mass damper", *Struct. Eng. Mech.*, **36**(2), 181-195.
Arrigan, J., Huang, C., Staino, A., Basu, B. and Nagarajaiah, S. (2014), "A frequency tracking semi-active algorithm for control of edgewise vibrations in wind turbine blades", *Smart Struct. Syst.*, **13**(2), 177-201.
Cheng, F.Y., Jiang, H. and Lou, K. (2008), *Smart Structures: Innovative Systems for Seismic Response Control*, CRC Press, U.S.A.
CAN/CSA-S16-09(2009), *Limit States Design of Steel Structures*, Canadian Standards Association.
Chey, M., Chase, J.G., Mander, J.B. and Carr, A.J. (2010), "Semi-active tuned mass damper building systems: Design", *Earthq. Eng. Struct. D.*, **39**(2), 119-139.
CISC, Handbook of Steel Construction, Tenth Edition (2011), Canadian Institute Of Steel Construction.
Chung, P.Y. Lin, L.L. and Loh, C.H. (2005), "Semi-active control of building structures with semi-active tuned mass damper", *Comput. - Aided Civil Infrastruct. E.*, **20(**1), 35-51.
El Kafrawy, O. Bagchi, A. and Humar, J. (2011), "Seismic performance of concrete moment resisting frame buildings in Canada", *Struct. Eng. Mech.*, **37**(2), 233-251.
Esteki, K., Bagchi, A. and Sedaghati, R. (2015), "Application of a semi-active tuned mass damper in controlling the seismic response of a building", *Proceedings of the 11th Canadian Conference in Earthquake Engineering (11 CCEE)*, Victoria, B.C.
Esteki, K., Bagchi, A. and Sedaghati.R. (2014), "Dynamic analysis of electro- and magneto-rheological fluid dampers using duct flow models", *Smart Mater. Struct.*, **23,** 035016 (11pp), DOI: 10.1088/0964-1726/23/3/035016.
Esteki, K., Bagchi, A. and Sedaghati, R. (2011), "A new phenomenological model for random loading of MR/ER damper", *Proceedings of the 2nd International Engineering Mechanics and Materials Specialty Conference*, Annual Conference of the Canadian Society of Civil Engineering, Ottawa, Canada.
CSI (2014), ETABS - Integrated Analysis, Design and Drafting of Building Systems; Computers and Structures Inc. (CSI) Berkeley, CA 94704 USA.
Ghaffarzadeh, H. (2013), "Semi-Active structural fuzzy Control with MR dampers subjected to near-fault ground motions having forward directivity and fling step", *Smart Struct. Syst.*, **12**(6), 595-617.
Hoang, N., Fujino, P. and Warnitchai, P. (2008), "Optimal tuned mass damper for seismic applications and practical design formulas", *Eng. Struct.*, **30(**3), 707-715.
Hrovat, D., Barak, P. and Rabins, M. (1983), "Semi-active versus passive or active tuned mass dampers for structural control", *J. Eng. Mech. - ASCE* , **109**(3), 691-705.
Jangid, R.S. (1995), "Dynamic characteristics of structures with multiple tuned mass dampers", *Struct. Eng. Mech.*, **3**(5), 497-509.
Ji, H.R., Moon, Y.J., Kim, C.H. and Lee, I.W. (2005), "Structural vibration control using semi-active tuned mass damper", *Proceedings of the 18th KKCNN Symposium on Civil Engineering-KAIST6*, Taiwan. ,
Jung, H.J., Spencer, B.F., Ni, Y.Q. and Lee, I.W. (2004), "State-of-the-art of semiactive control systems using MR fluid dampers in civil engineering applications", *Struct. Eng. Mech.*, **17**(3), 493-526.
Koo, J. H. (2003), *Using magneto-rheological dampers in semi-active tuned vibration absorbers to control structural vibrations*, Ph.D. Dissertation, Virginia Polytechnic Institute and State University, Virginia, U.S.A.
Liedes, T. (2010), *Improving the performance of the semi-active tuned mass damper*, Ph.D. Dissertation, University of Oulu, Oulu, Finland.
Marano, G.C. and Greco, R. (2010), "Optimization criteria for tuned mass dampers for structural vibration control under stochastic excitation", *J, Vib. Control*, **17**(5), 679-688.
MATLAB (R2011a), Math Works Inc, Massachusetts, U.S.A.
NBCC (2010), National Building Code of Canada, National Research Council, Ottawa, Canada.
Ogata, K. (2010), *Modern Control Engineering*, International Edition 5th Ed., Pearson.
Ormondroyd, J. and Den Hartog, J.P. (1928), "The theory of the dynamic vibration absorber", *J. Appl. Mech. - ASME*, **50**, 9-22.

Pinkaew, T. and Fujino, Y. (2001), "Effectiveness of semi-active tuned mass dampers under harmonic excitation", *Eng. Struct.*, **23**(7), 850-856.
Rana, R. and Soong, T. (1998), "Parametric study and simplified design of tuned mass dampers", *Eng. Struct.*, **20**(3), 193-204.
Runlin, Y., Xiyuan, Z. and Xihui, L. (2002), "Seismic structural control using semi-active tuned mass dampers", *Earthq. Eng. Eng. Vib.*, **1**(1), 111-118.
Sadek, F., Mohraz, B., Taylor, A. and Chung, R. (1997), "A method of estimating the parameters of tuned mass dampers for seismic applications", *Earthq. Eng. Struct. D.*, **26**(6), 617-635.
Setareh, M. (2001), "Application of semi-active tuned mass dampers to base-excited systems", *Earthq. Eng. Struct. D.*, **30**(3), 449-462.
Mathworks (2011a), Matlab-R2011a, The MathWorks, Inc., Natick, Massachusetts, United States.
Mathworks (2011b), Simulink-R2011a,The MathWorks, Inc., Natick, Massachusetts, United States.
Sadek, F., Mohraz, B., Taylor, A. and Chung, R. (1997), "A method of estimating the parameters of tuned mass dampers for seismic applications", *Earthq. Eng. Struct. D.*, **26**(6), 617-635.
PEER (2013), The Pacific Earthquake Engineering Research Center, Ground motion database, http://peer.berkeley.edu/
Watakabe, M., Tohdo, M., Chiba, O., Izumi, N., Ebisawa, H. and Fujita, T. (2001), "Response control performance of a hybrid mass damper applied to a tall building", *Earthq. Eng. Struct. D.*, **30**(11), 1655-1676.
Warburton, G.B. (1982), "Optimum absorber parameters for various combinations of response and excitation parameters", *Earthq. Eng. Struct. D.*, **10**(3), 381-401.
Yang, F., Esmailzadeh, E. and Sedaghati, R. (2010), "Optimal vibration suppression of structures under random base excitation using semi-active mass damper", *J. Vib. Acoust.*, **132**(4), 041002 (10pp).
Yang, G., Spencer, B.F., Carlson, J.D. and Sain, M.K. (2002), "Large-scale MR fluid dampers: modeling and dynamic performance considerations", *Eng. Struct.*, **24**(3), 309-323.
Ying, Z.G., Ni, Y.Q. and Ko, M. (2009), "A semi-active stochastic optimal control strategy for nonlinear structural systems with MR dampers", *Smart Struct. Syst.*, **5**(1), 69-79.
Yousuf, M. and Bagchi, A. (2010), "Seismic performance of a twenty storey steel frame building in Canada", *J. Struct. Des. Tall Spec. Build.*, **19**, 901-921.

CC